



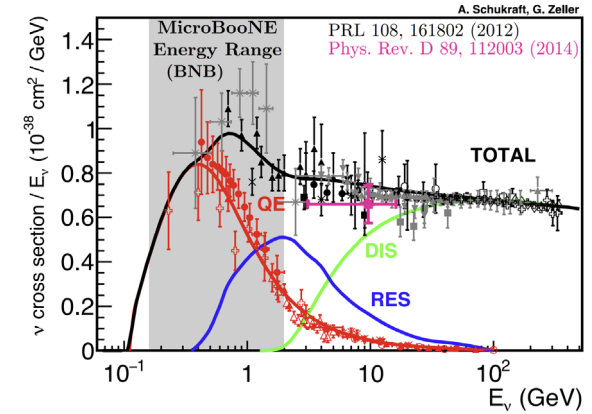
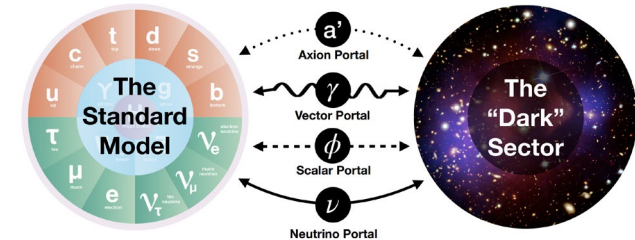
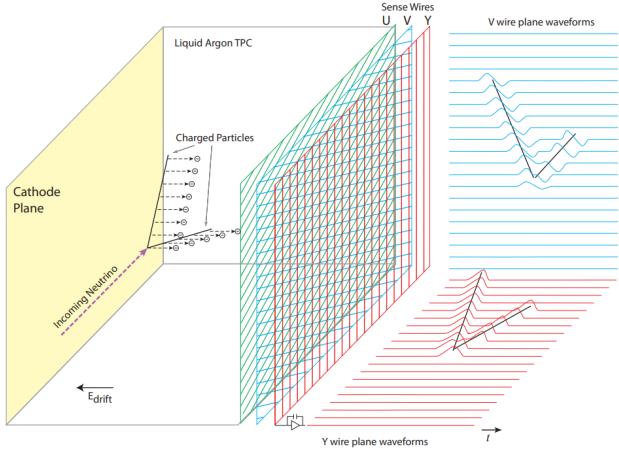
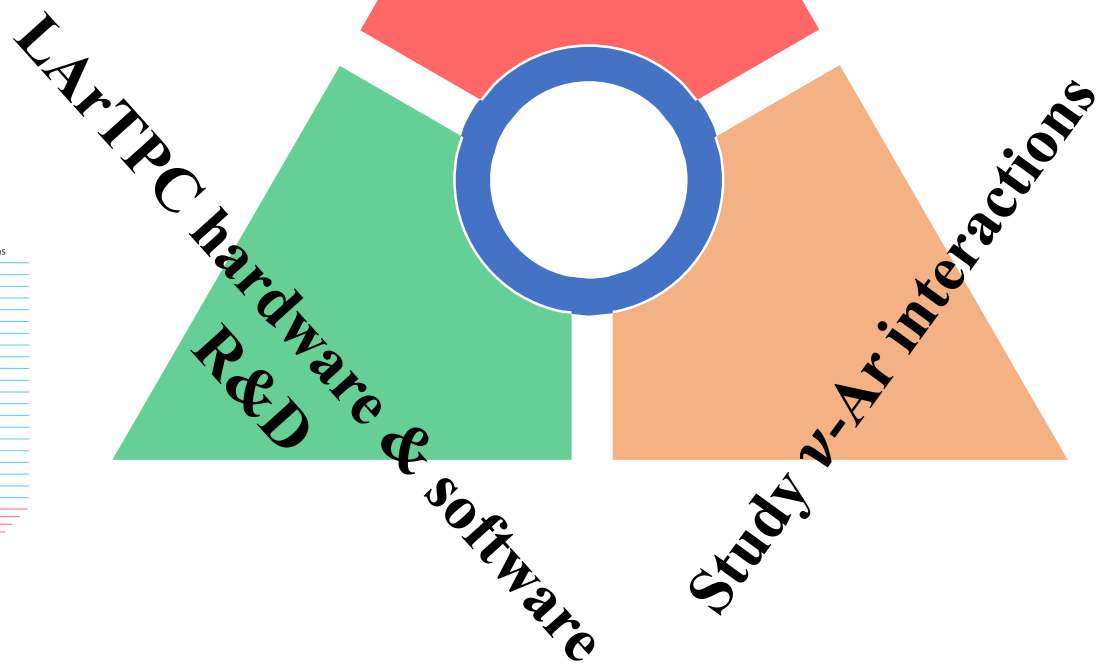
Recent Results from MicroBooNE's Search *for a Low-Energy-Excess Anomaly under the Electron Hypothesis and additional BSM Studies*

Xiangpan Ji (Nankai University)
On behalf of the MicroBooNE Collaboration

TAUP 2025, August 25, Xichang

MicroBooNE Scientific Goals

Investigate MiniBooNE Low Energy Excess
Search for BSM physics



MicroBooNE Scientific Goals

81
papers

2025

2024

2023

2022

2021

2020

2019

2018

2017
2016

Measurement of charged-current muon neutrino-argon interactions without pions in the final state using the MicroBooNE detector
 First study of neutrino angle reconstruction using quasielastic-like interactions in MicroBooNE
 First measurement of ν_e and $\bar{\nu}_e$ charged current single charged pion production differential cross sections on argon using the MicroBooNE detector
 First Measurement of Charged Current Muon Neutrino-Induced K^* Production on Argon using the MicroBooNE Detector
 First Search for Dark Sector e^+e^- Explanations of the MiniBooNE Anomaly at MicroBooNE
 Inclusive Search for Anomalous Single-Photon Production in MicroBooNE
 First Search for Neutral Current Coherent Single-Photon Production in MicroBooNE
 Enhanced Search for Neutral Current Asymmetries Single-Photon Production in MicroBooNE
 Study of Neutral Current Asymmetries in Quasielastic Interactions in MicroBooNE
 Search for Neutral Current Asymmetries in Quasielastic Interactions in MicroBooNE - Analysis Using Data and Monte-Carlo Simulations
 Data-driven model validation for neutrino-nucleus cross section measurements
 Demonstration of new MeV-scale capabilities in large neutrino-LArTPCs using electron, positron, and cosmogenic activity in MicroBooNE
 Demonstration of neutron identification with LArTPC detectors
 Improving neutrino energy estimation of neutrino interactions in LArTPCs using electron and positron scattering
 First double-differential cross section measurement of neutral-current π^0 production in neutrino-argon scattering in the MicroBooNE detector
 Measurement of the differential cross section for neutral pion production in charged-current muon neutrino interactions on argon with the MicroBooNE detector
 Measurement of double-differential cross sections for mesonless charged-current muon neutrino interactions on argon with final-state protons using the MicroBooNE detector
 First Simultaneous Measurement of Differential Muon-Neutrino Charged-Current Cross Sections on Argon for Final States with and Without Protons Using MicroBooNE Data
 Inclusive cross section measurements in final states with and without protons for charged-current ν_e -Ar scattering in MicroBooNE
 First Search for Dark-Trident Processes Using the MicroBooNE Detector
 Search for Heavy Neutral Leptons in Electron-Positron and Neutral-Ar Final States with the MicroBooNE Detector
 Measurement of nuclear effects in neutrino-argon interactions using a generalized kinematic imbalance technique with the MicroBooNE detector
 First application of liquid argon time projection chamber for the search for a rare nuclear neutrino-atom scattering and annihilation $\nu_n \rightarrow e^-$ using the MicroBooNE detector
 Measurement of three-dimensional inclusive muon-neutrino charged-current cross sections on argon with the MicroBooNE detector
 Measurement of ambient argon decay rates and energy spectra from liquid argon using the MicroBooNE detector
 First Measurement of η Nucleon Production in Neutrino Interactions on Argon with MicroBooNE
 First demonstration of QFS instability in the MicroBooNE liquid argon time projection chamber
 Multidifferential cross section measurement of neutrino-argon quasielastic-like reactions with the MicroBooNE detector
 First Double-Differential Measurement of Kinetic Instability in Neutrino Interactions with the MicroBooNE Detector
 First Measurement of Quasielastic A Barium Imbalance in Muon-Arte-Argon Interactions in the MicroBooNE Detector
 First Measurement of Differential Cross Section in Muon Neutrino Charged Current Interactions on Ar-40 with MicroBooNE
 First Constraints on Light Sterile Neutrino Oscillations from Charged Current and Coherence Searches in MicroBooNE
 Search for Non-Lived Heavy Neutral Leptons and Higgs Bosons via Coherence and Decay in the MicroBooNE detector
 Differential Cross Section Measurement of Charged Current Events in Liquid Argon in MicroBooNE
 Measurement of neutral current single π^0 production on argon with the MicroBooNE detector
 Observation of radon mitigation in MicroBooNE by a liquid argon filter
 Novel approach for evaluating detector-related uncertainties in a LArTPC using MC simulation and real data
 Search for an Excess of Electron Neutrino Interactions in MicroBooNE Using Quasielastic Final State Topologies
 Whole-cell 3D pattern recognition techniques for neutrino event reconstruction
 Search for low energy atmospheric neutrino oscillations via a flux-dependent method using MicroBooNE
 Search for atmospheric neutrino oscillations via a flux-dependent method using MicroBooNE
 Search for atmospheric neutrino oscillations using a background subtraction method in MicroBooNE
 Search for atmospheric neutrino oscillations using a background subtraction method in MicroBooNE
 Search for atmospheric neutrino oscillations using a background subtraction method in MicroBooNE
 Search for atmospheric neutrino oscillations in MicroBooNE using a background subtraction method
 Search for atmospheric neutrino oscillations in MicroBooNE using a background subtraction method
 Measurement of the longitudinal effective interaction length in MicroBooNE
 Measurement of the longitudinal effective interaction length in MicroBooNE using liquid argon
 Measurement of the longitudinal effective interaction length in MicroBooNE using argon gas
 Measurement of the atmospheric neutrino rate with the MicroBooNE liquid Argon Time Projection Chamber
 Measurement of the atmospheric neutrino rate with the MicroBooNE liquid Argon Time Projection Chamber
 The continuous medium effect in the MicroBooNE liquid argon time projection chamber for reduction of superneutrino neutrinos
 Measurement of space charge effects in the MicroBooNE liquid Argon Time Projection Chamber
 Generic Segmentation with Sparse Convolutional Network for Event Reconstruction in MicroBooNE
 A Convolutional Neural Network for Reconstruction of the MicroBooNE Liquid Argon Time Projection Chamber
 Performance Evaluation of the MicroBooNE Liquid Argon Time Projection Chamber With CERN's R&D Imaging and Design Optics Modules
 Event Type Reconstruction for the MicroBooNE Liquid Argon Time Projection Chamber
 Identification of Muon-Neutrino Interactions in MicroBooNE
 Identification of Muon-Neutrino Interactions in MicroBooNE
 Identification of Muon-Neutrino Interactions in MicroBooNE
 Identification of Muon-Neutrino Interactions in MicroBooNE

LArTPC hardware & software

Study ν -Ar interactions

My talk today



the Micro Booster Neutrino Experiment (MicroBooNE)

*185 Collaborators
from 41 Institutions*

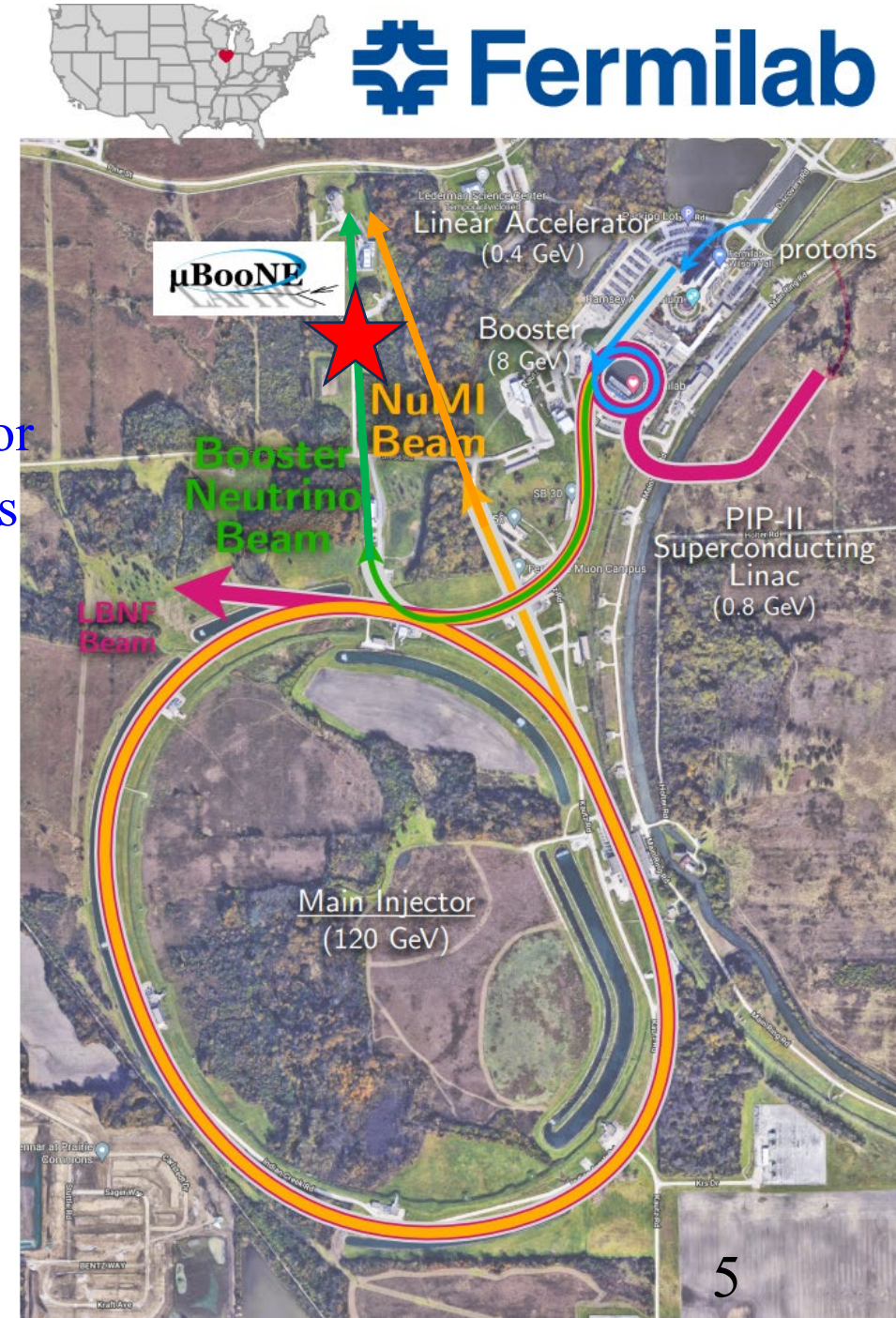
MicroBooNE



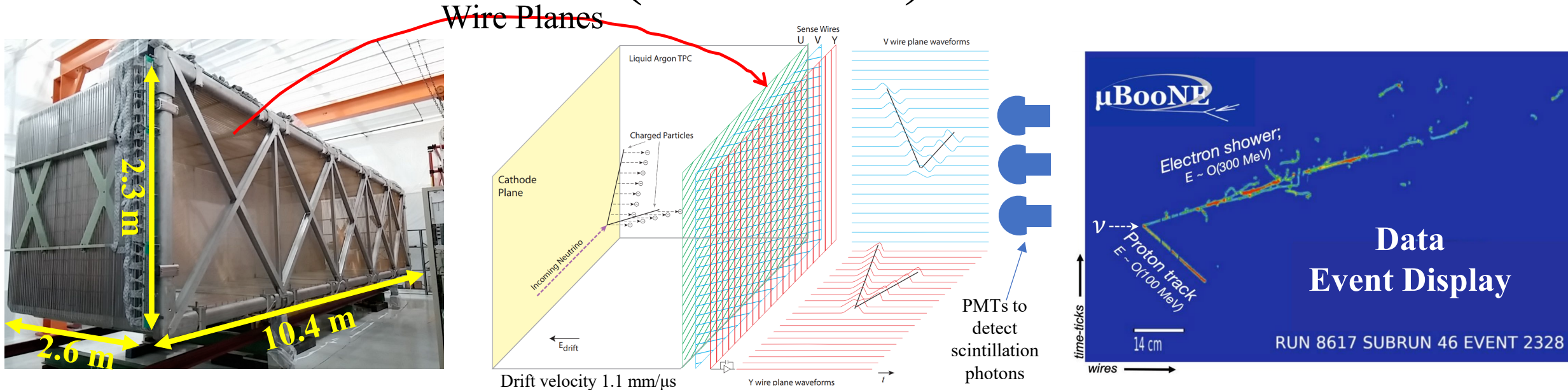
- Located at Fermilab
- Surface-level LArTPC detector
- 85 ton active liquid Argon mass
- Took data: 2015-2021
- Decommissioned now

Two Neutrino Beams

On-axis beam: BNB	Off-axis (8°) beam: NuMI
8 GeV protons	120 GeV protons
470 meter baseline	~680 meter baseline
0.8 GeV mean neutrino E	1.5 GeV mean neutrino E
Collected ~0.5M neutrino events	~0.3M neutrino events



Liquid Argon Time Projection Chamber (LArTPC)



Full-Active Tracking Calorimeter

- mm-level position resolution
- MeV-level detection energy threshold
- ns-scale neutrino interaction time resolution
- 3D reconstruction of position

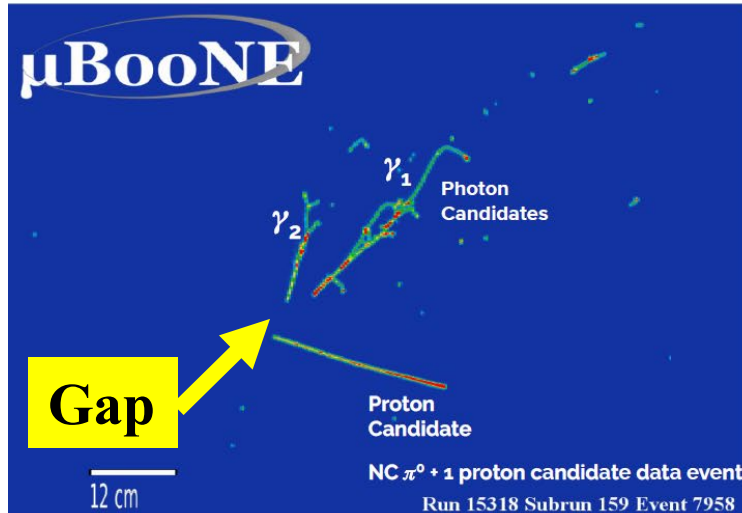
<https://microboone.fnal.gov/documents-publications/>

Excellent Particle Identification

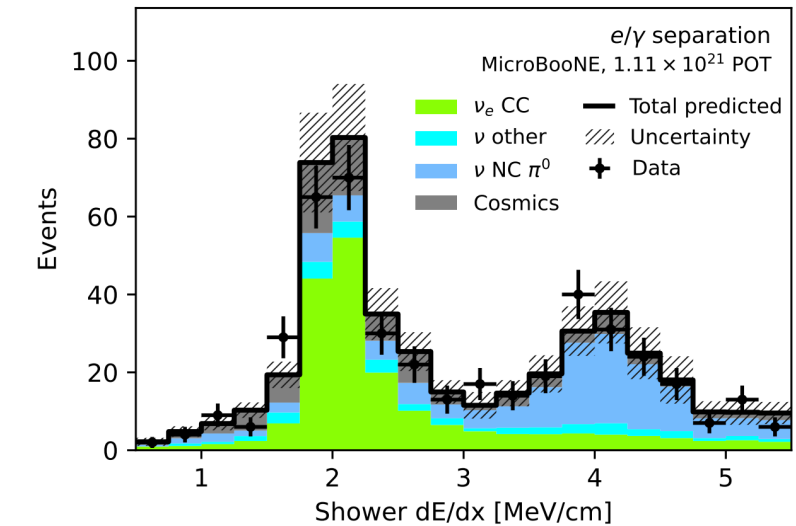
- Final states topological and calorimetric
- Track and shower identification
- Electron and photon shower separation
- Distinguish muons, protons, pions

Electron and Photon shower Separation

Gap between shower start point and ν vertex



Electron 1-MIP vs. photon 2-MIPs

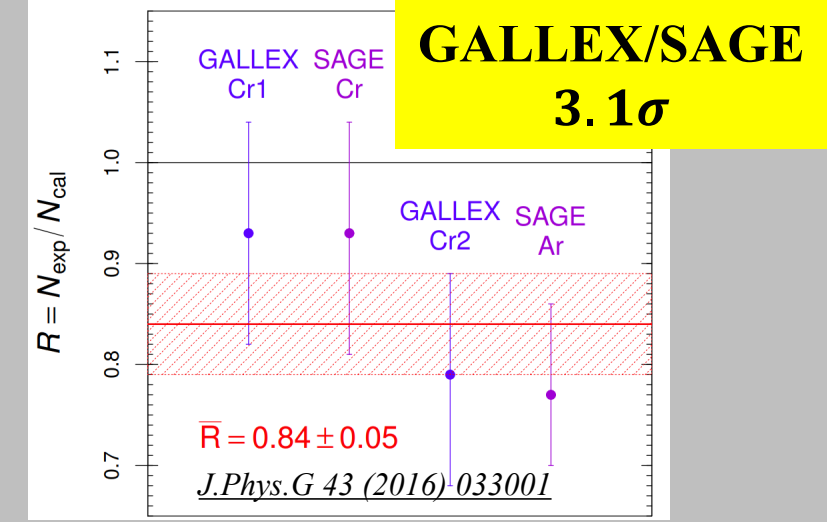
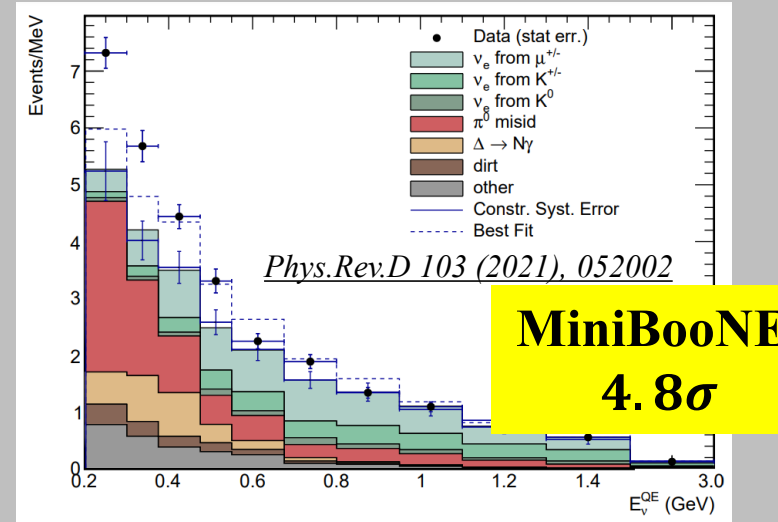
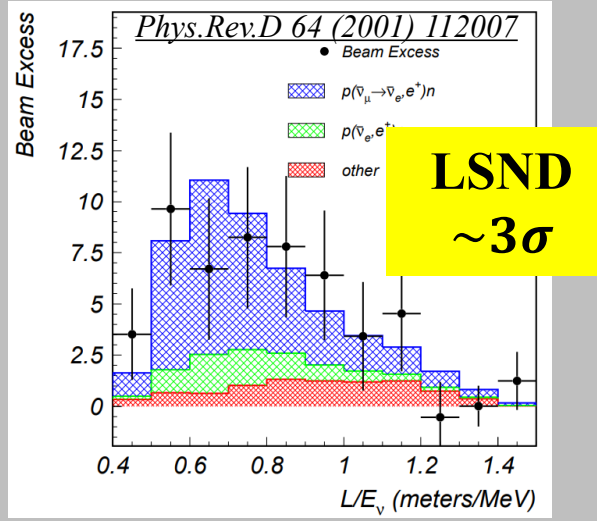
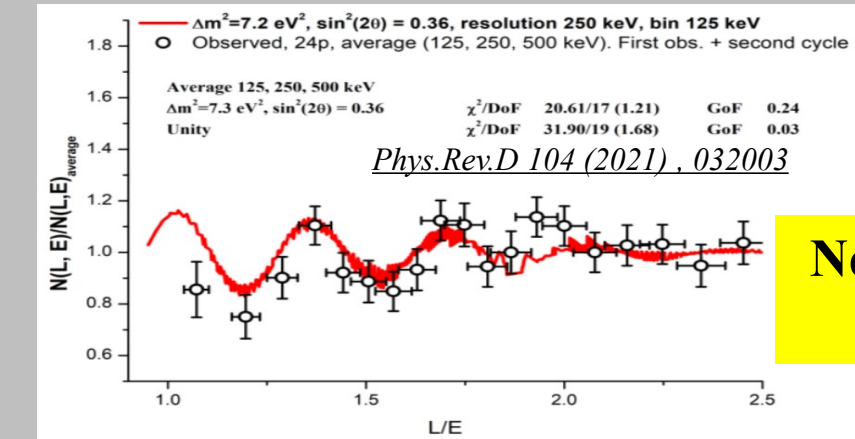
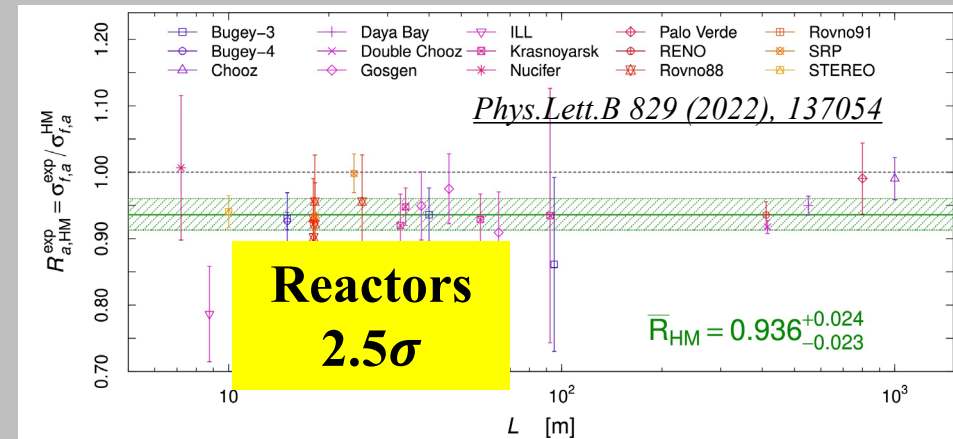


Full-Active Tracking Calorimeter

- mm-level position resolution
- MeV-level detection energy threshold
- ns-scale neutrino interaction time resolution
- 3D reconstruction of position

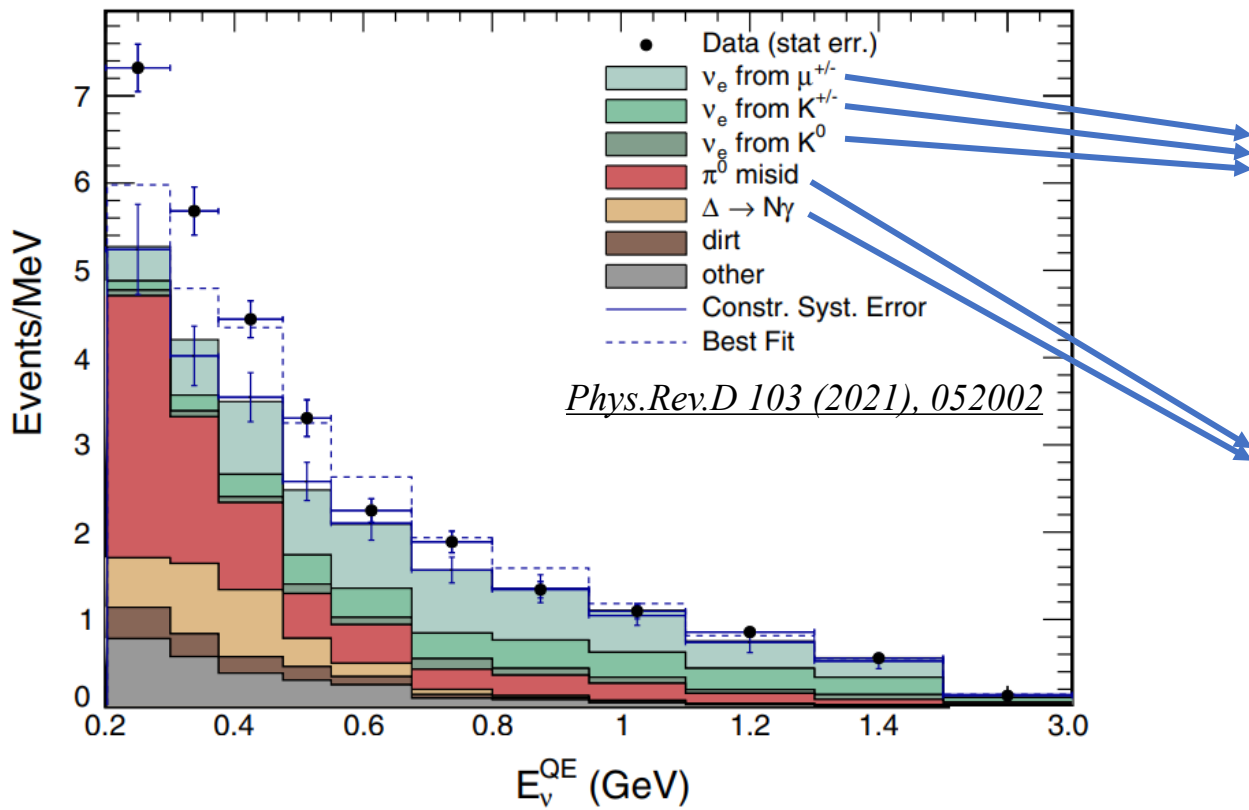
Excellent Particle Identification

- Final states topological and calorimetric
- Track and shower identification
- Electron and photon shower separation
- Distinguish muons, protons, pions

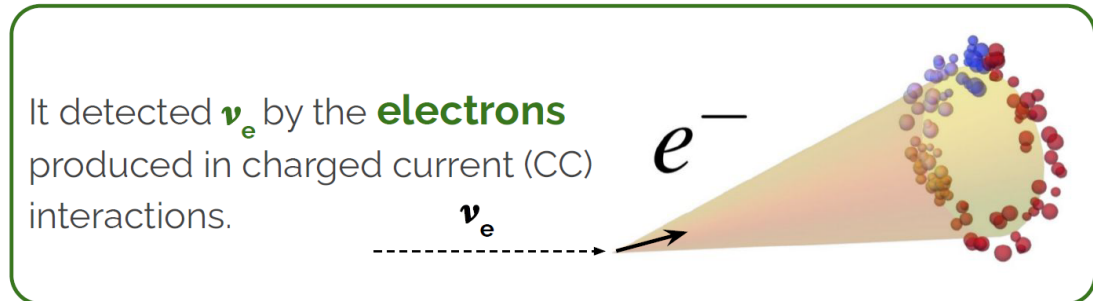


Short-Baseline Neutrino Anomalies -- Hints of eV-Scale Neutrinos

MiniBooNE Anomaly: Low Energy Excess (LEE) eLEE or gLEE



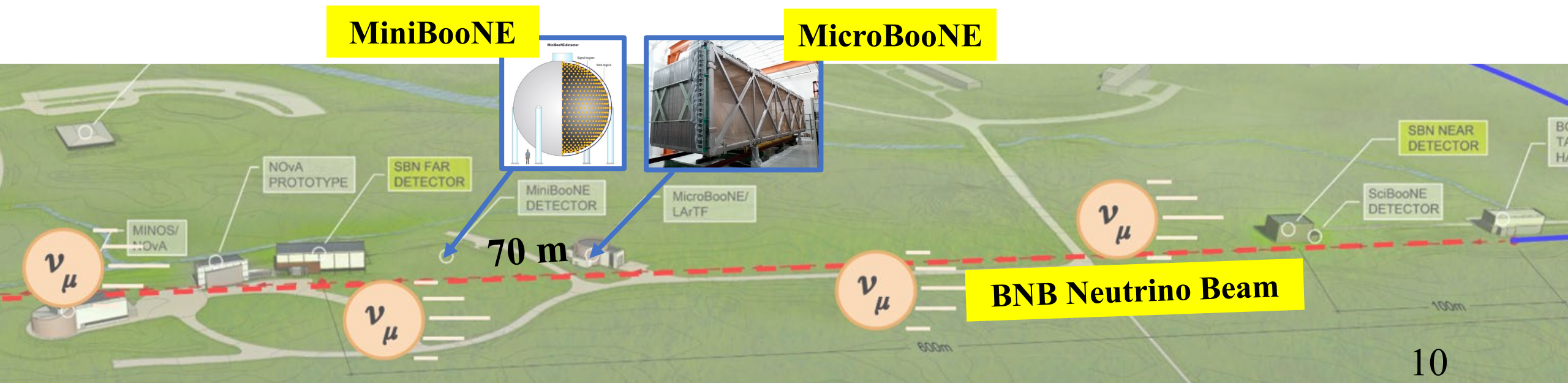
MiniBooNE (2002-2019) observed the LEE of electromagnetic events with 4.8σ significance.



MiniBooNE Cherenkov detector unable to distinguish photons and electrons, and unable to detect hadronic final-state particles below Cherenkov threshold.

MicroBooNE: eLEE Investigation

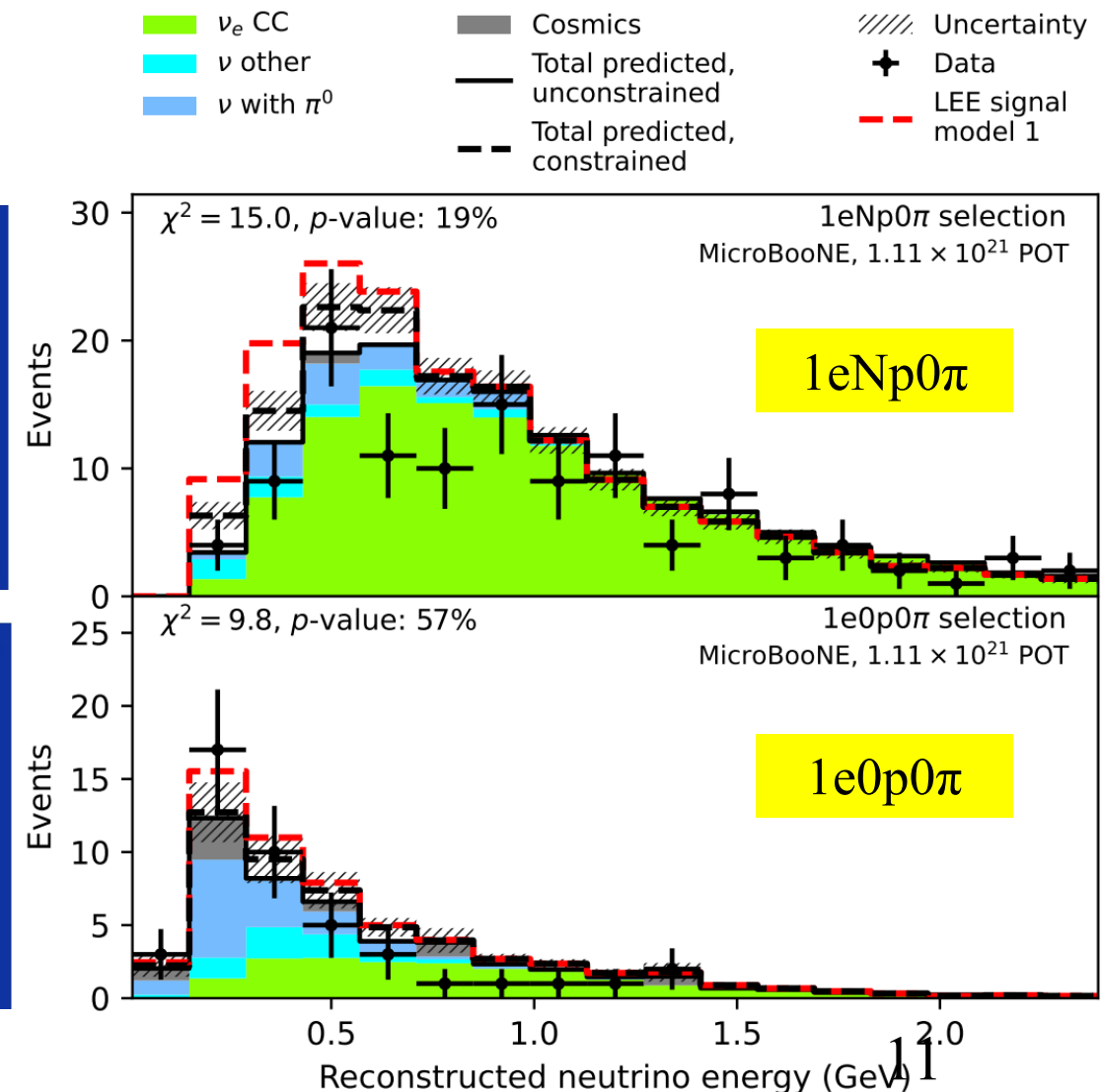
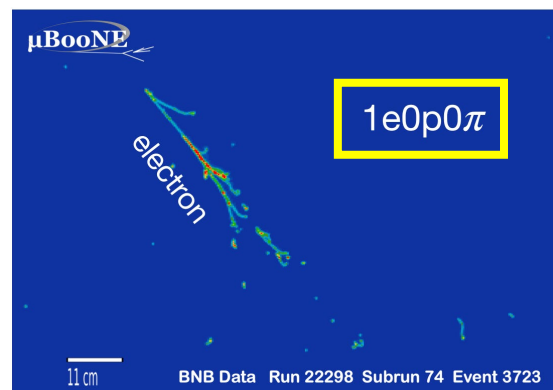
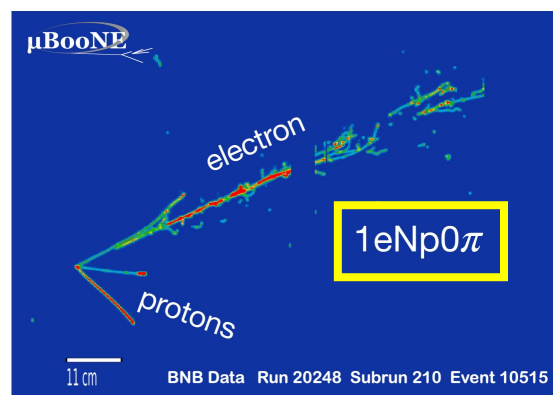
- First round results, data taken between 2016.2 – 2018.6 *Phys. Rev. Lett. 128, 241801 (2022)*
 - ν_e CC final states analysed: (1) 1e1p, (2) 1eNp0 π and 1e0p0 π , (3) inclusive 1eX
 - (1)(2)(3) with different reconstruction techniques
- Latest results, full five-year operation dataset 2016 – 2020 *Phys. Rev. Lett. 135, 081802 (2025)*
08/21/2025
 - ν_e CC final states analysed: 1eNp0 π and 1e0p0 π
 - Multiple LEE models tested: neutrino energy, shower kinematics

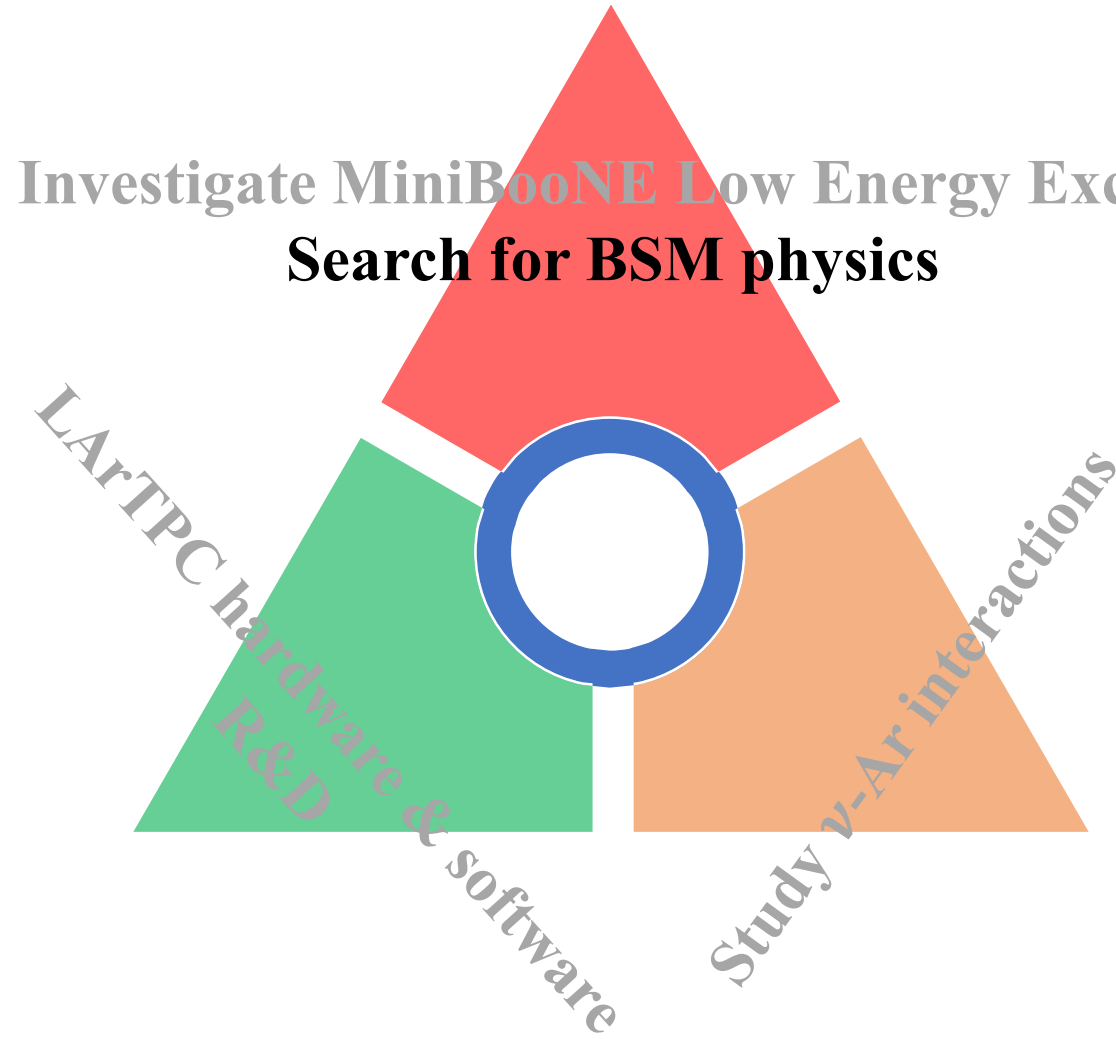


MicroBooNE: eLEE Investigation

Phys. Rev. Lett. 135, 081802 (2025)

- Investigated ν_e CC with no pions in the MicroBooNE full BNB dataset
- See no sign of MiniBooNE-like excess
- Exclude MiniBooNE LEE as ν_e at $\geq 99\%$ CL
- Confirmed our previous eLEE search results





3(active)+1(sterile) Neutrino Oscillation Framework

Look at 3+1 model

$$\begin{pmatrix} \nu_e \\ \nu_\mu \\ \nu_\tau \\ \nu_s \end{pmatrix} = \begin{pmatrix} U_{e1} & U_{e2} & U_{e3} & U_{e4} \\ U_{\mu 1} & U_{\mu 2} & U_{\mu 3} & U_{\mu 4} \\ U_{\tau 1} & U_{\tau 2} & U_{\tau 3} & U_{\tau 4} \\ U_{s1} & U_{s2} & U_{s3} & U_{s4} \end{pmatrix} \begin{pmatrix} \nu_1 \\ \nu_2 \\ \nu_3 \\ \nu_4 \end{pmatrix}$$

$$P_{\nu_\alpha \rightarrow \nu_\beta} = \delta_{\alpha\beta} + (-1)^{\delta_{\alpha\beta}} \sin^2(2\theta_{\alpha\beta}) \sin^2\left(\frac{\Delta m_{41}^2 L}{4E_\nu}\right)$$

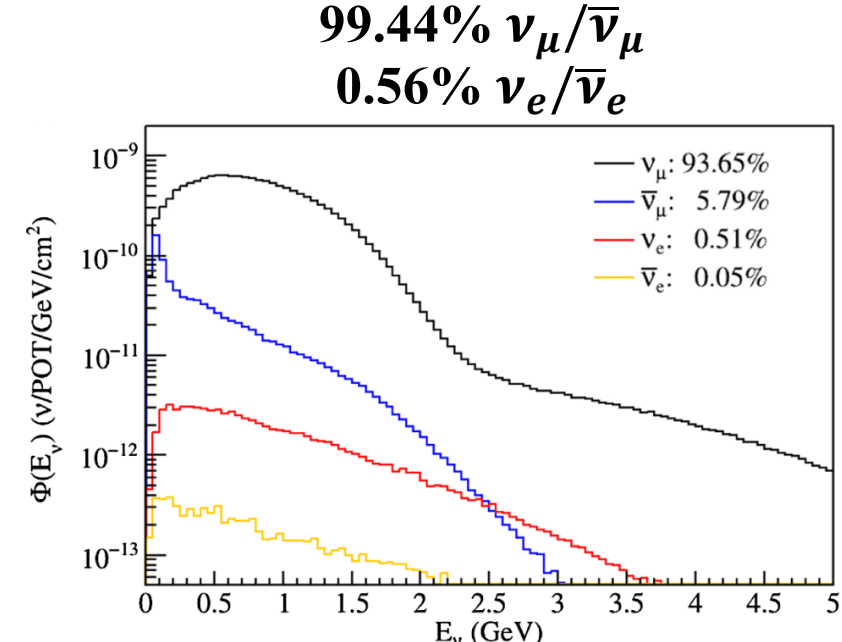
$$\nu_e \text{ disappearance } (\nu_e \rightarrow \nu_e): \sin^2 2\theta_{ee} = \sin^2 2\theta_{14}$$

$$\nu_e \text{ appearance } (\nu_\mu \rightarrow \nu_e): \sin^2 2\theta_{\mu e} = \sin^2 2\theta_{14} \sin^2 \theta_{24}$$

$$\nu_\mu \text{ disappearance } (\nu_\mu \rightarrow \nu_\mu): \sin^2 2\theta_{\mu\mu} = 4 \cos^2 \theta_{14} \sin^2 \theta_{24} (1 - \cos^2 \theta_{14} \sin^2 \theta_{24})$$

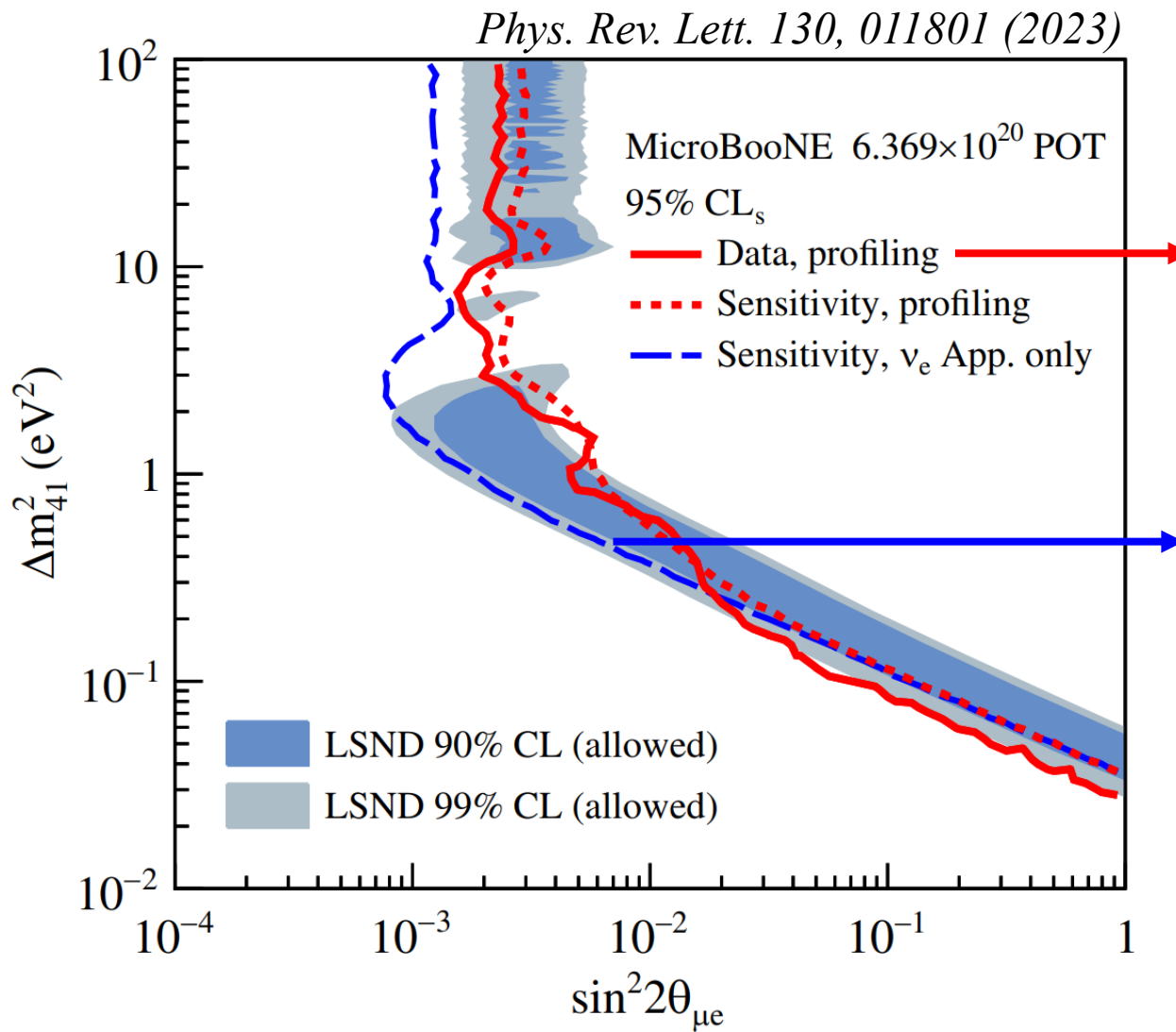
Quantitatively probes $\frac{L(m)}{E_\nu(\text{MeV})} \sim \mathcal{O}(1)$ oscillation feature, and search for eV-scale sterile neutrinos.

BNB beam @ MicroBooNE
Mean Neutrino Energy 0.8 GeV



3+1 Sterile Neutrino Oscillations

Results by using BNB data



- 2D profiled result, full 3+1 analysis at each point in the parameter space.
- Oscillation effects considered:

$$\nu_\mu \rightarrow \nu_e$$

$$\nu_e \rightarrow \nu_e$$

$$\nu_\mu \rightarrow \nu_\mu$$

- ν_e appearance-only, more stringent limit However, it is physically not allowed in the 3+1 framework. (non-zero ν_e appearance requires both ν_e and ν_μ disappearance)
- Oscillation effects considered:

$$\nu_\mu \rightarrow \nu_e$$

3+1 Sterile Neutrino Results

Limited by the Cancellation of ν_e Appearance and Disappearance

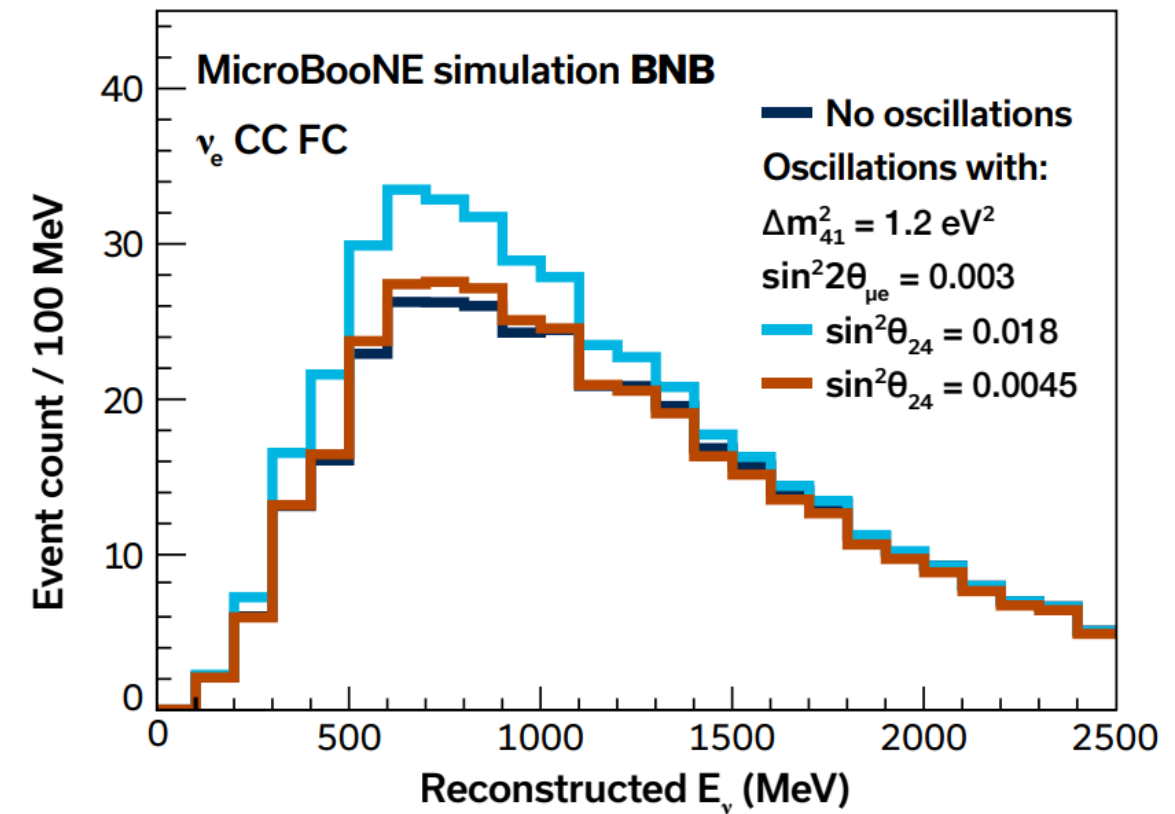
- Observed ν_e events are a combination result of ν_e appearance and disappearance

$$N_{\nu_e} = N_{\text{intrinsic } \nu_e} \cdot P_{\nu_e \rightarrow \nu_e} + N_{\text{intrinsic } \nu_\mu} \cdot P_{\nu_\mu \rightarrow \nu_e}$$

$$= N_{\text{intrinsic } \nu_e} \cdot [1 + (R_{\nu_\mu/\nu_e} \cdot \sin^2 \theta_{24} - 1) \cdot \sin^2 2\theta_{14} \cdot \sin^2 \Delta_{41}]$$

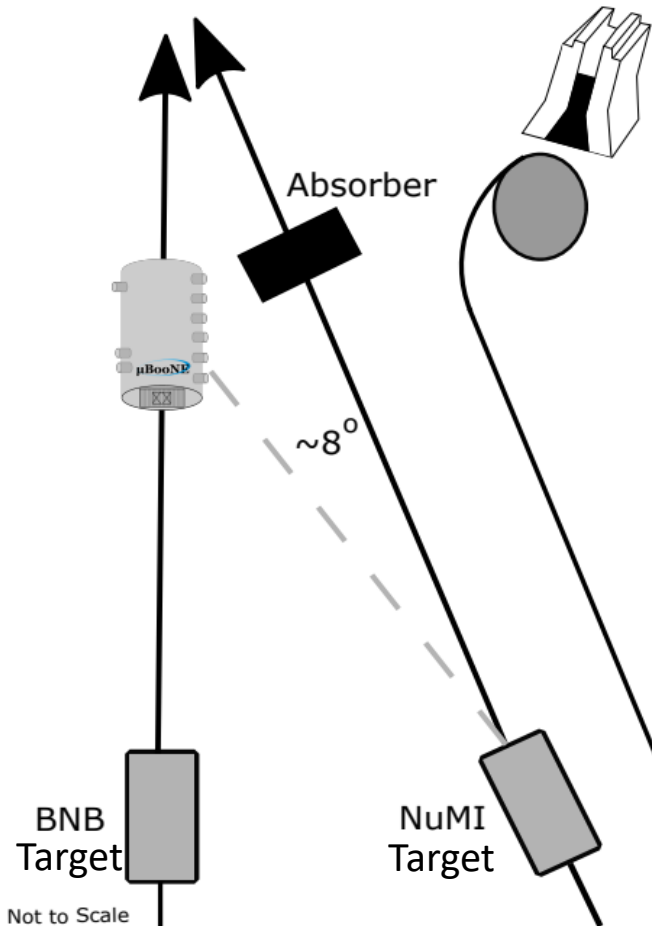
- Degeneracy when $\sin^2 \theta_{24}$ approaches R_{ν_e/ν_μ} (the ratio of beam intrinsic ν_e and ν_μ flux)

At MicroBooNE	R_{ν_e/ν_μ} Average
BNB beam	~ 0.005



One Detector with Two Beams

Breaking the Cancellation of ν_e App. and Disapp.

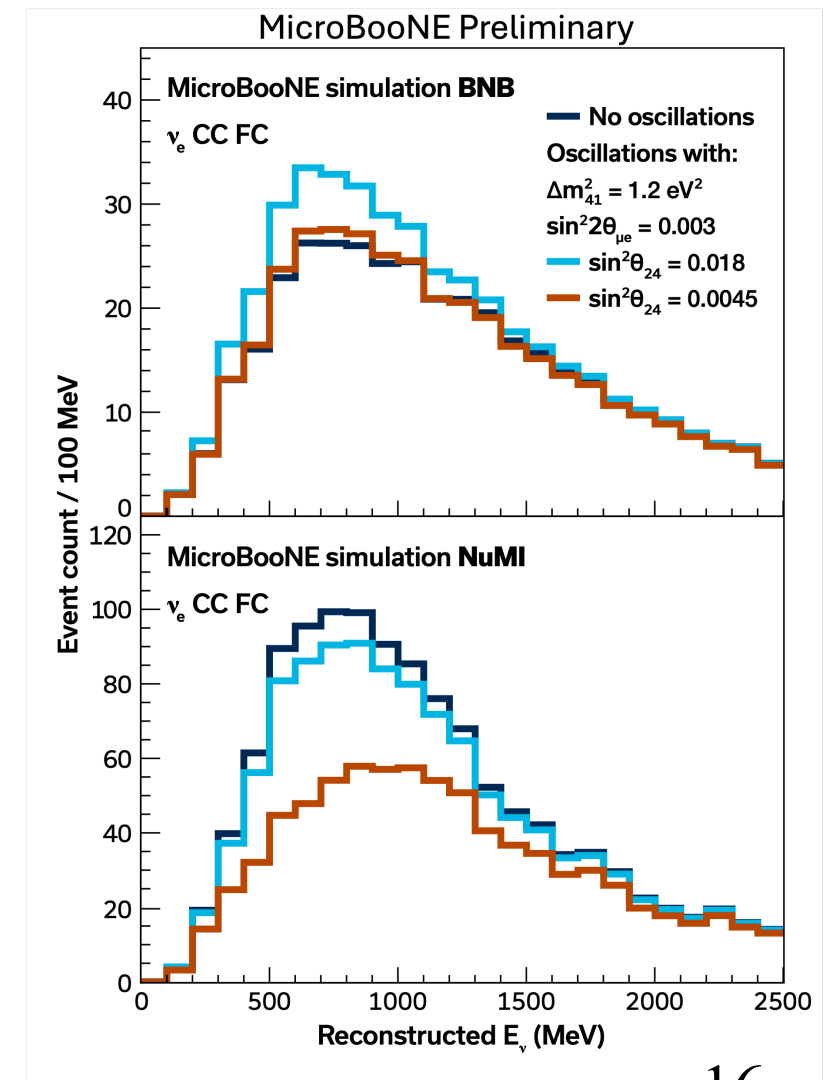


$$\begin{aligned}
 N_{\nu_e} &= N_{\text{intrinsic } \nu_e} \cdot P_{\nu_e \rightarrow \nu_e} + N_{\text{intrinsic } \nu_\mu} \cdot P_{\nu_\mu \rightarrow \nu_e} \\
 &= N_{\text{intrinsic } \nu_e} \cdot \left[1 + (R_{\nu_\mu/\nu_e} \cdot \sin^2 \theta_{24} - 1) \cdot \sin^2 2\theta_{14} \cdot \sin^2 \Delta_{41} \right]
 \end{aligned}$$

- Degeneracy when $\sin^2 \theta_{24}$ approaches R_{ν_e/ν_μ} (the ratio of beam intrinsic ν_e and ν_μ flux)

At MicroBooNE	R_{ν_e/ν_μ} Average
BNB beam	~0.005
NuMI beam	~0.04

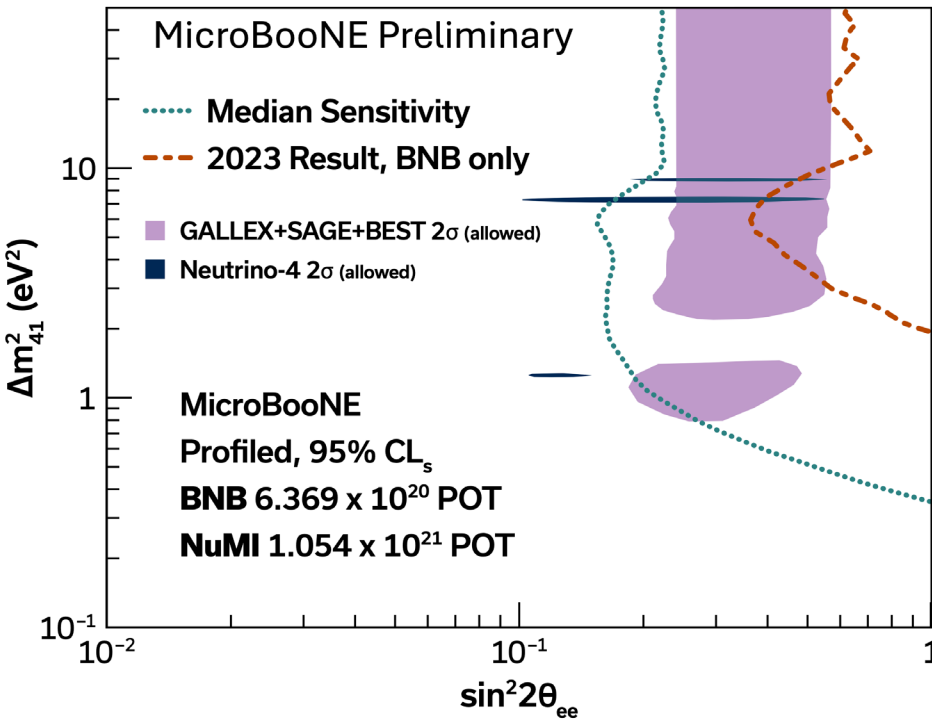
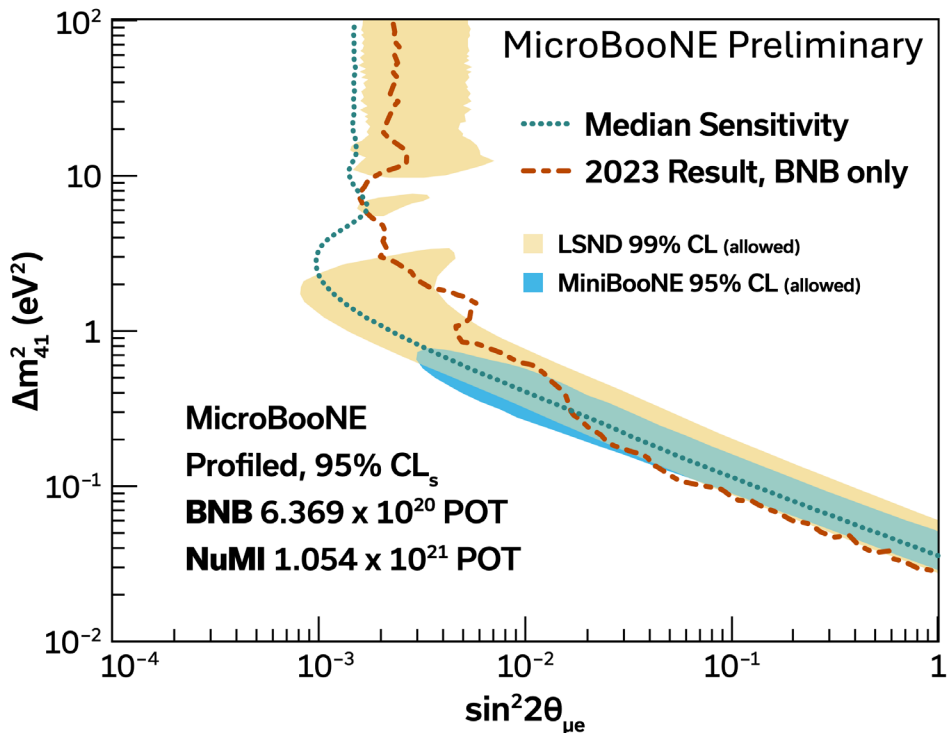
Significant difference in the ν_μ/ν_e flux ratio in BNB and NuMI
 → mitigate the degeneracy



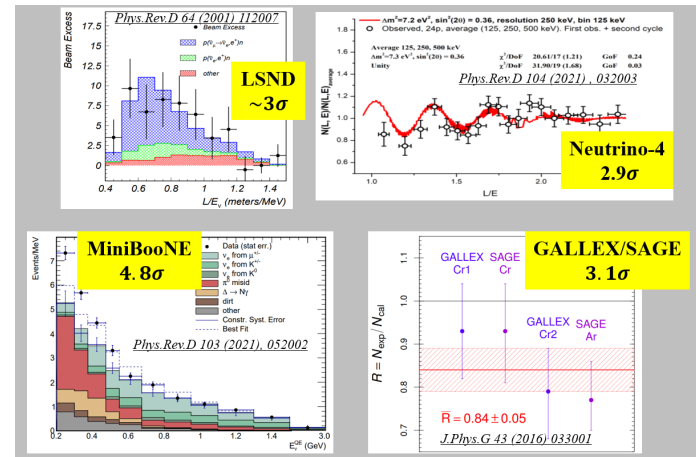
3+1 Sterile Neutrino Oscillations

BNB+NuMI

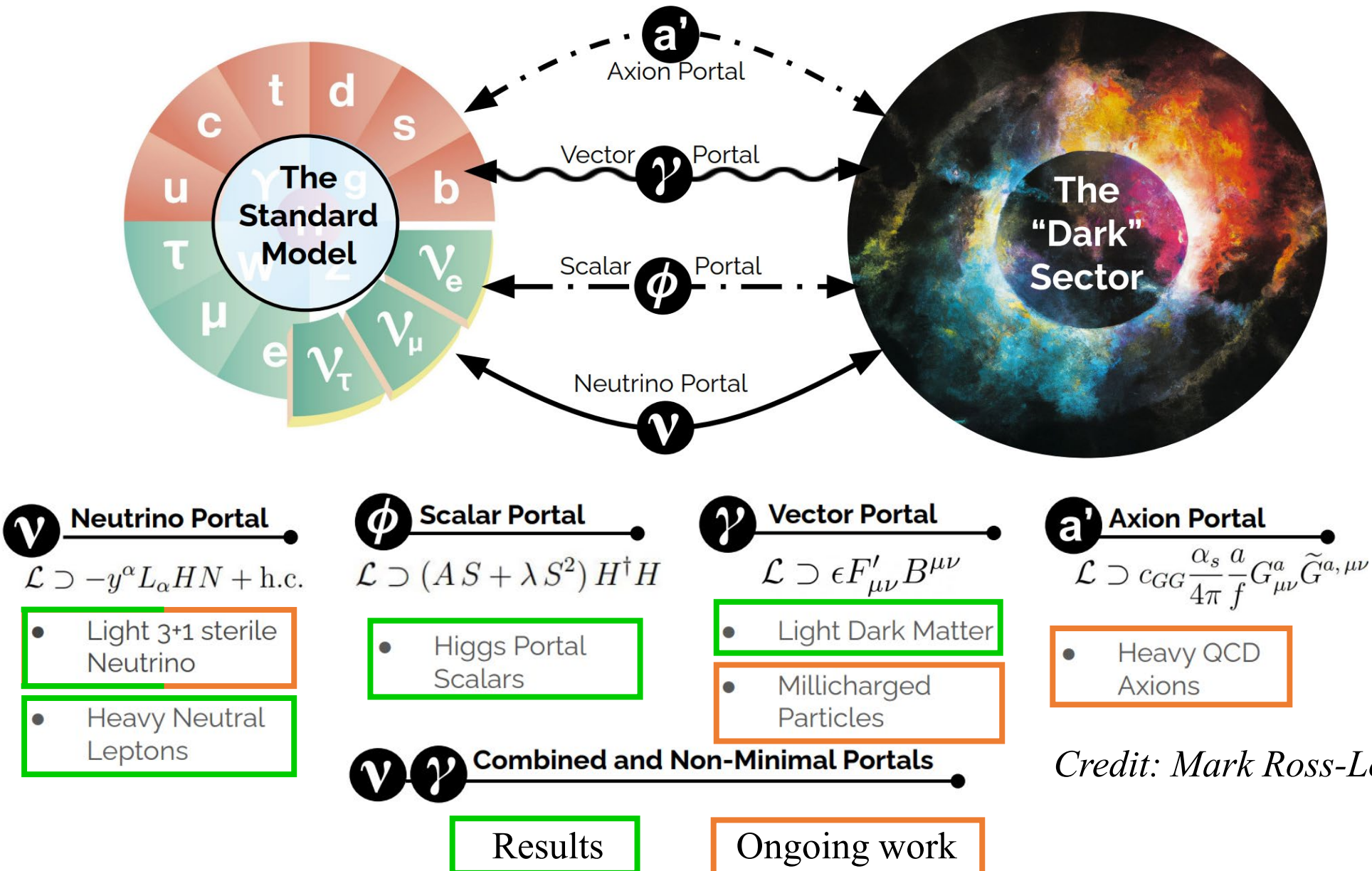
Adding second beam (NuMI) largely improves the sensitivities for both $\nu_\mu \rightarrow \nu_e$ and $\nu_e \rightarrow \nu_e$ channels. Great coverage across LSND/MiniBooNE, GAA/Neutrino-4 allowed regions.



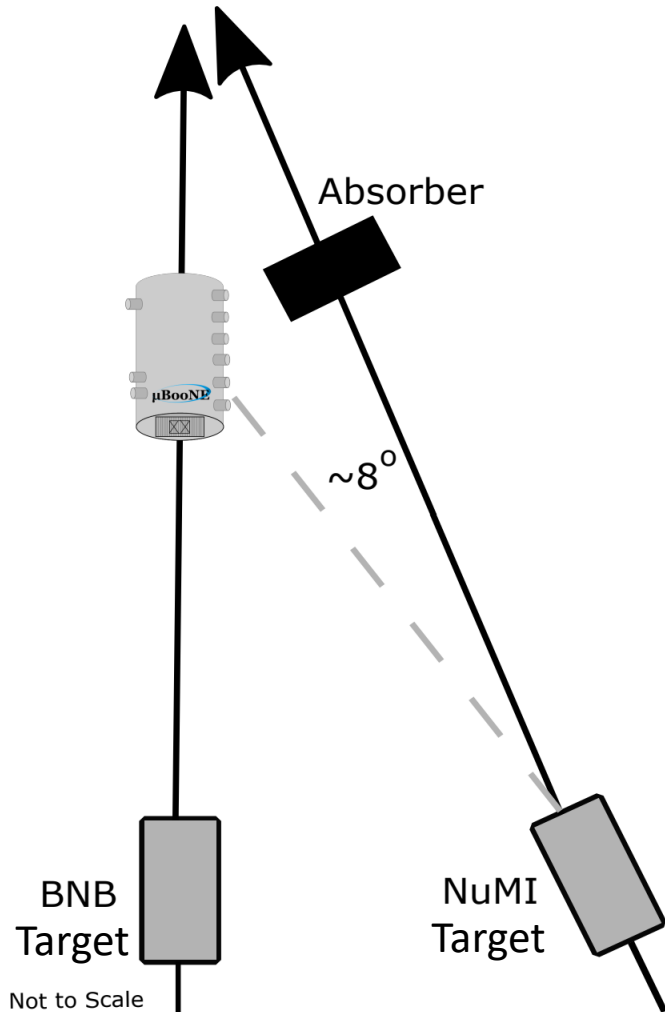
Data Results Out Soon!



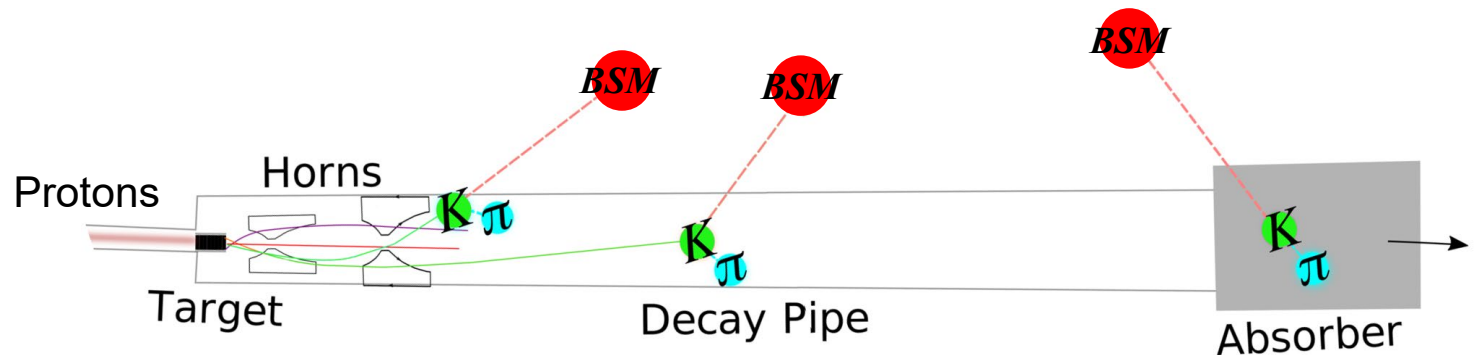
Portals to the Dark Sector



A Source for BSM Particles



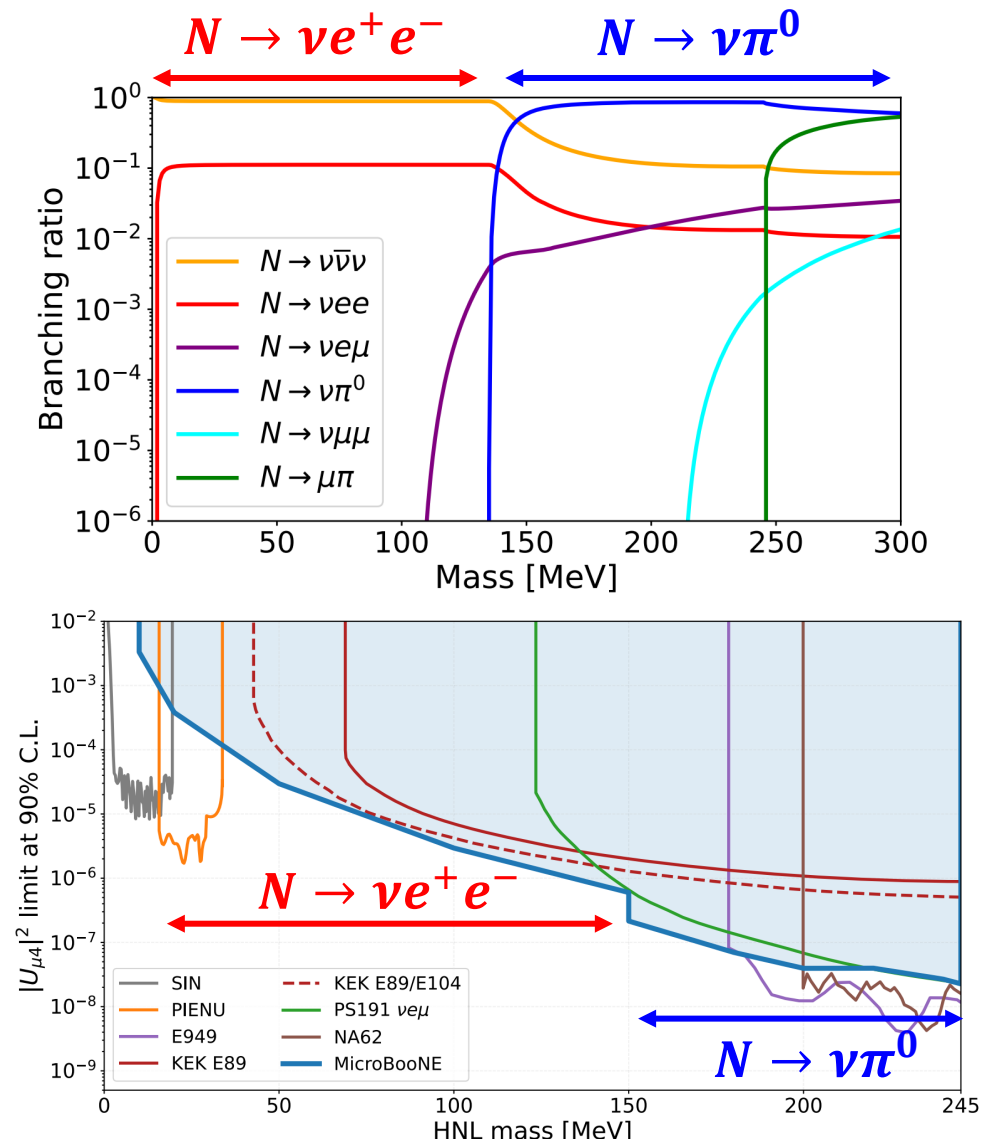
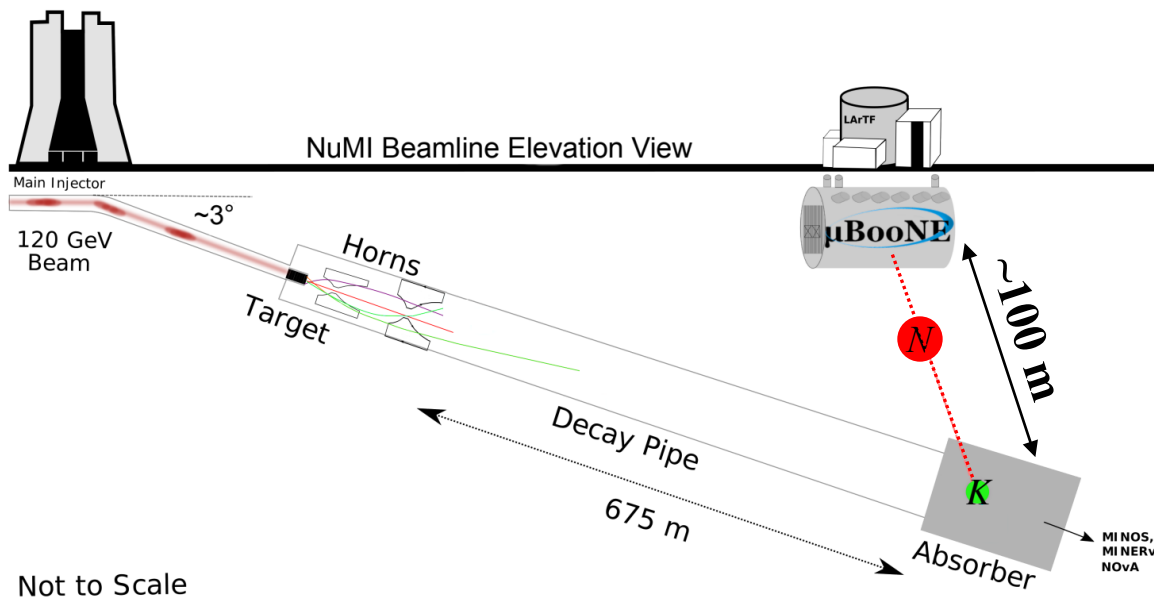
- Collisions with the target produce amounts of mesons
- Some models have mechanisms by which charged and neutral mesons can decay into BSM particles
 - Decay at rest in the target region
 - Decay in flight in the decay region
 - Decay at rest in the absorber region
- These BSM particles may survive long enough to reach MicroBooNE detector



Heavy Neutral Leptons (HNL)

Phys. Rev. Lett. 132, 041801 (2024)

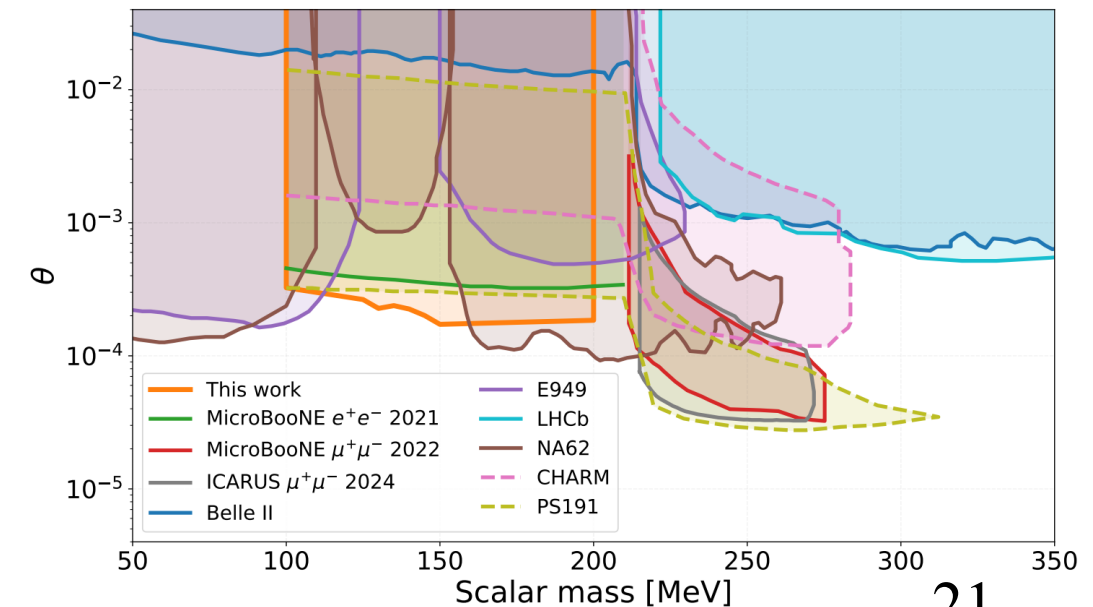
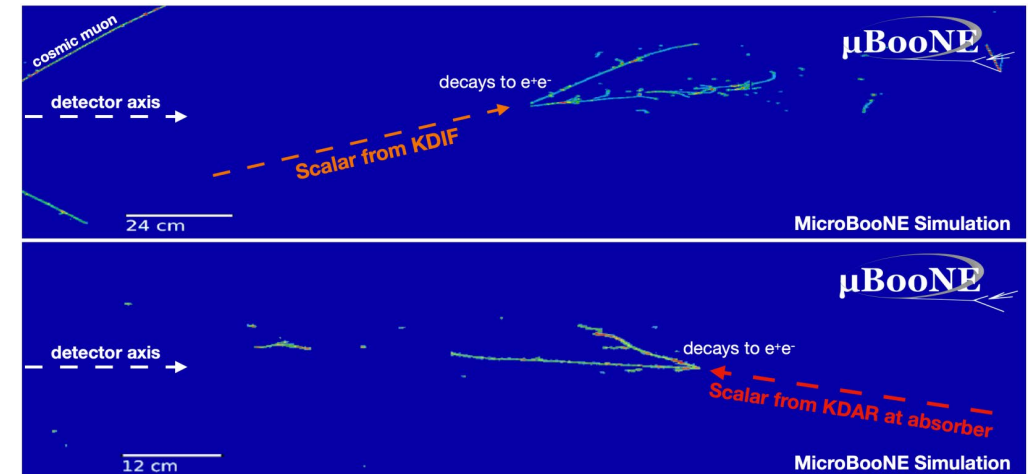
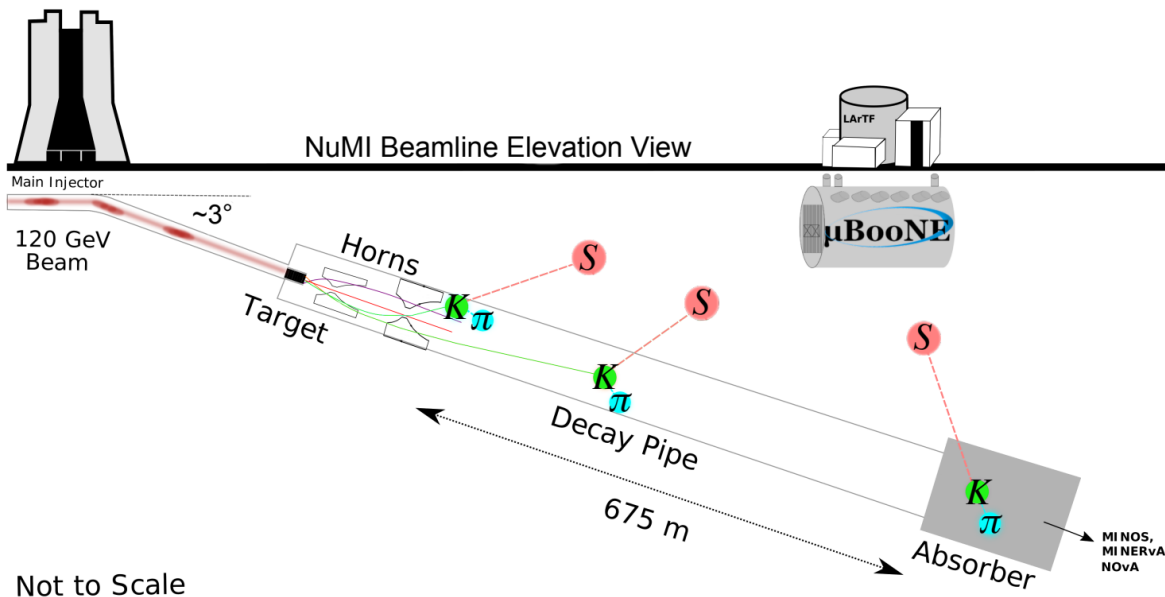
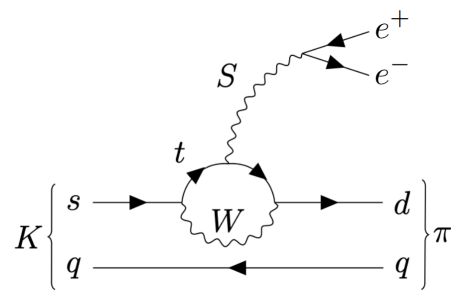
- HNLs produced from
 $K^+ \rightarrow \mu^+ N$ at NuMI absorber
- Searches for
 $N \rightarrow \nu e^+ e^-$
 $N \rightarrow \nu \pi^0$
- Set limits on $|U_{\mu 4}|^2$ as a function of HNL mass



Higgs-Portal Scalar Bosons

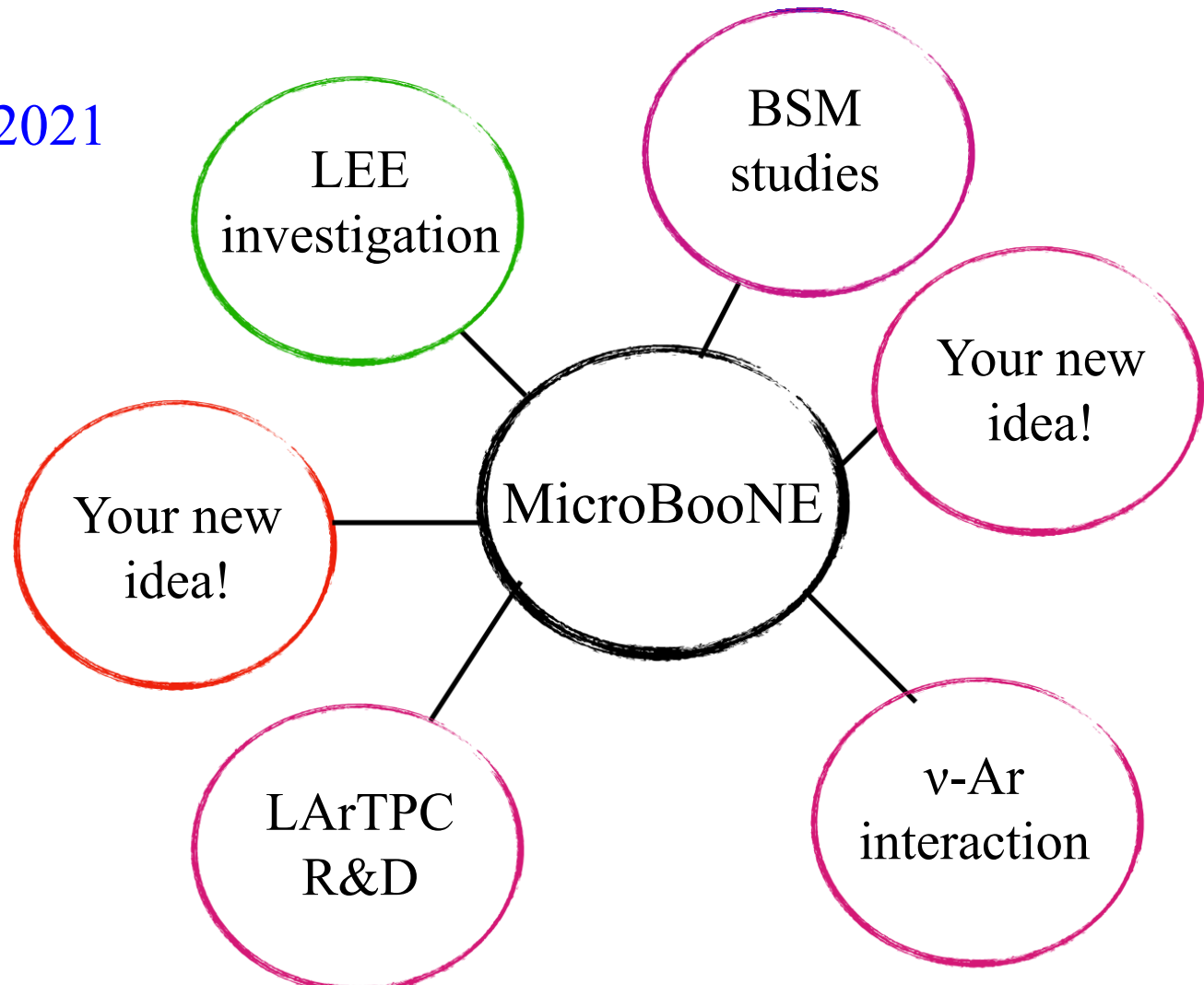
arXiv:2501.08052

- Neutral scale singlet S , mixing angle θ with Higgs boson
- Production from charged kaon decay
- Signature: $S \rightarrow e^+ e^-$
- Set strongest limits on θ to date for m_s at (125, 150) MeV



Summary

- MicroBooNE completed data taking 2015-2021
BNB and NuMI neutrino beams
- Extensive inclusive physics programs
- Many new full dataset analyses upcoming!



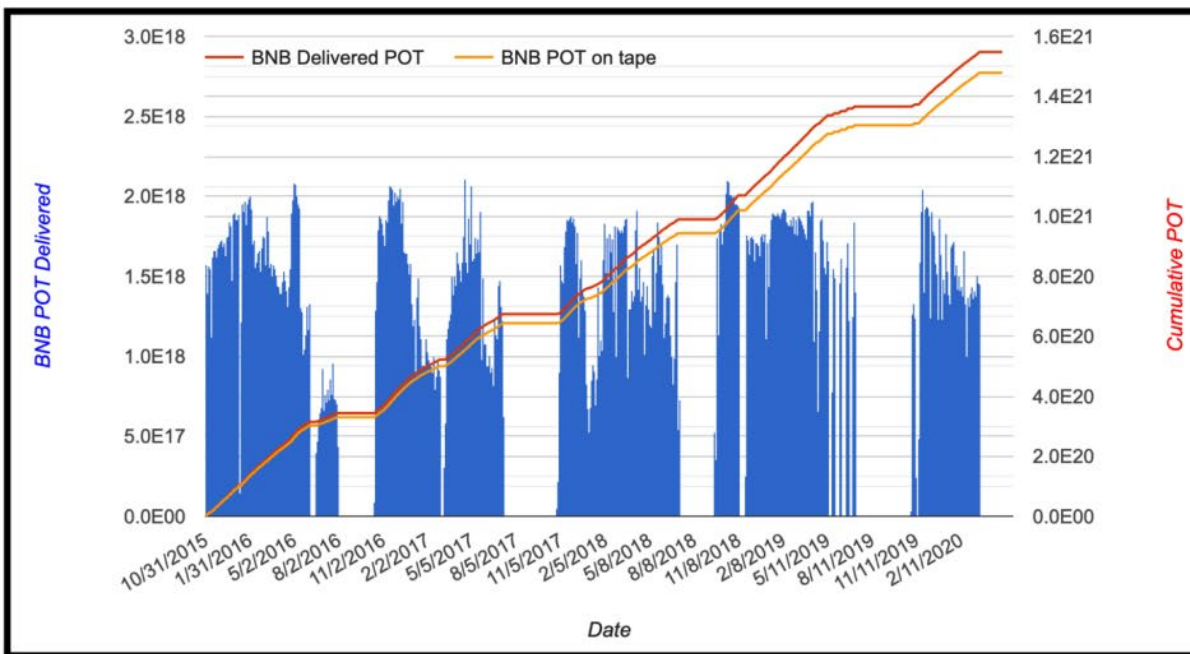


Thank you!

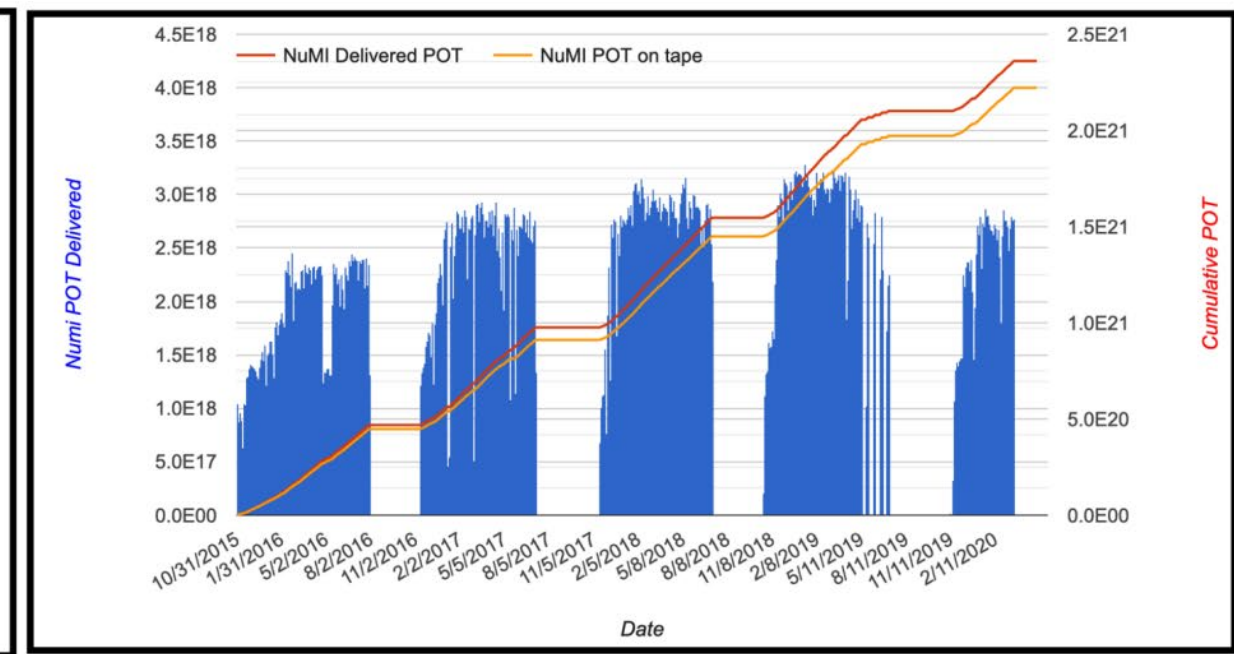
Backup

MicroBooNE Data Taking

On-axis BNB:
full dataset, 1.1×10^{21} POT



On-axis BNB:
full dataset, 2.37×10^{21} POT



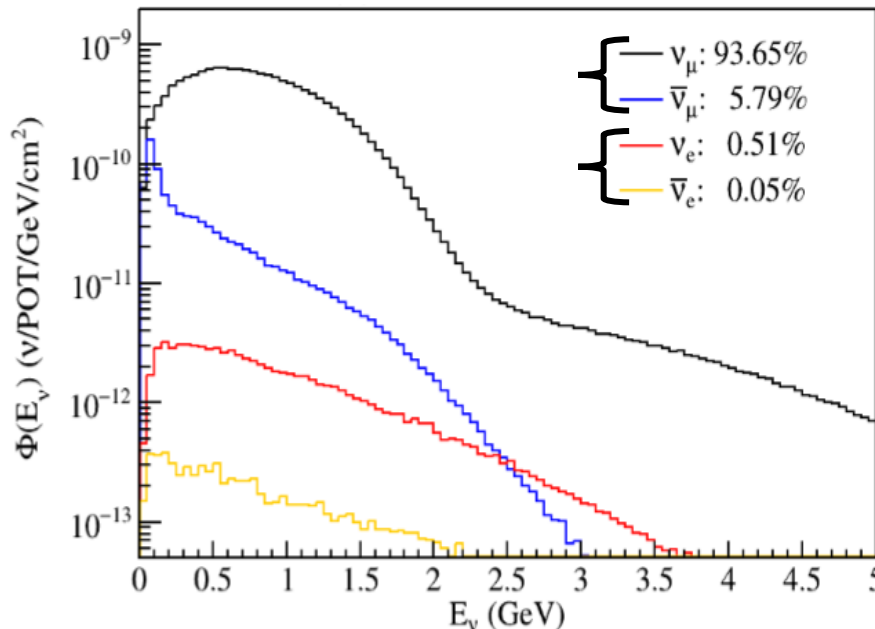
MicroBooNE collected data between 2015 and 2021 split into five runs.

Challenging ν_e Selection

Cosmic-ray muon (5.5 kHz)
@ MicroBooNE operating
near-surface



BNB neutrino flux
over 99% $\nu_\mu / \bar{\nu}_\mu$
 $\sim 0.5\% \nu_e / \bar{\nu}_e$

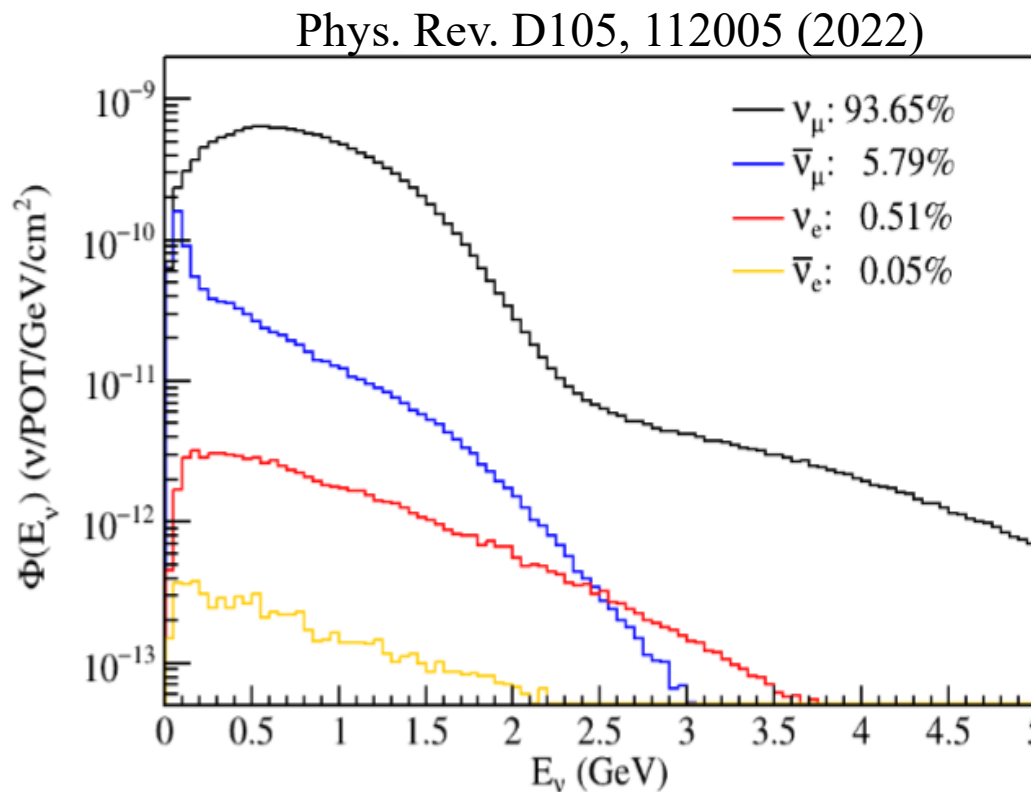


A sensitive ν_e selection (CC interactions) requires
 $\gtrsim 99.999\%$ rejection of cosmic-ray muons and
 $\gtrsim 99.9\%$ rejection of other ν background for nue analysis

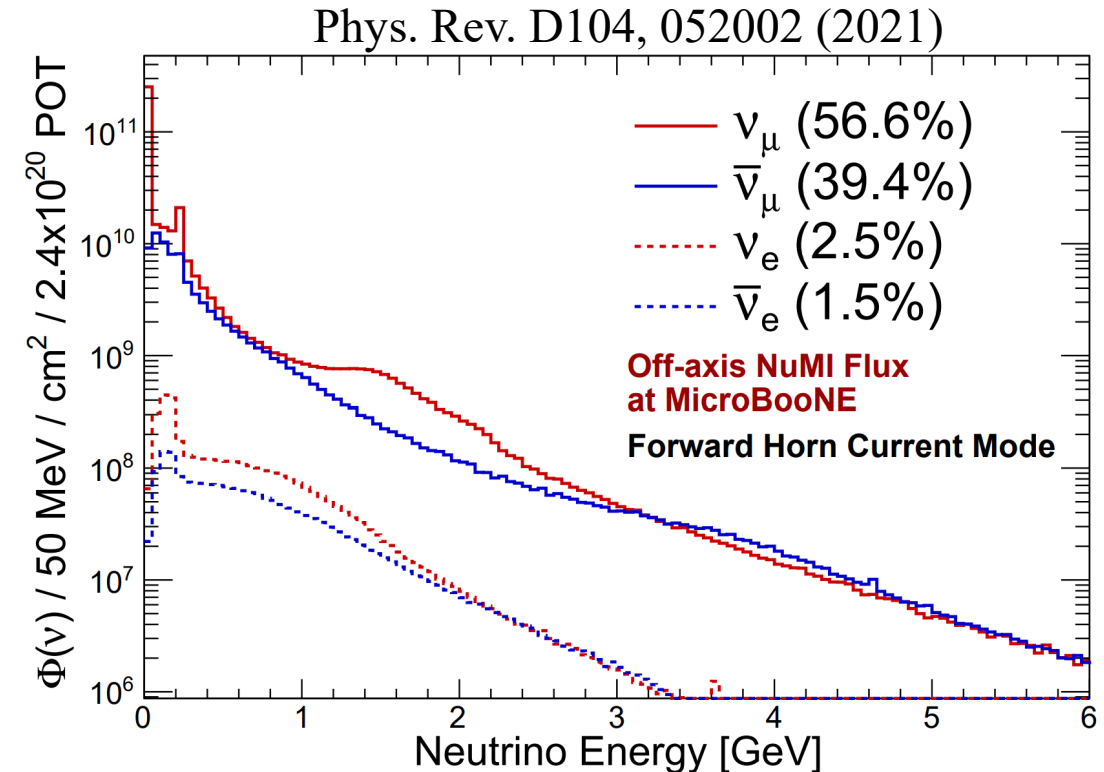
Developed advanced cosmic rejection techniques, event reconstruction and PID algorithms to exploit LArTPC capability to select ν_e events

BNB and NuMI Neutrino Flux @ MicroBooNE

BNB



NuMI



3+1 Sterile Neutrino Oscillations

Results by using BNB data

Phys. Rev. Lett. 130, 011801 (2023)

